Relay optics for enhanced Integral Imaging

Raul Martinez-Cuenca[1], Genaro Saavedra[1], Bahram Javidi[2] and Manuel Martinez-Corral[1]

[1]Department of Optics, University of Valencia, E-46100 Burjassot, Spain.
[2]Electrical and Computer Engineering Dept, University of Connecticut, Storrs, CT 06269-1157

ABSTRACT

Integral imaging provides with three-dimensional (3D) images. This technique works perfectly with incoherent light and does not need the use of any special glasses nor stabilization techniques. Here we present relay systems for both acquire and display 3D images. Some other important challenges are revisited.

Keywords: Integral imaging, 3D imaging display, digital processing.

1. INTRODUCTION

Integral Imaging (InI) is a 3D-imaging technique which is based on the Integral Photography[1]. Recently, InI has tackled the attention of many investigators[2-6] since its performance is still restricted by a set of drawbacks.

InI 3D imaging is achieved in two steps, namely, the pickup (or recording) and the display stages (see Fig. 1). We propose the use of relay systems in both stages as a first step to solve some of this drawbacks. We analyze the imaging properties of InI systems to point out the fundamental challenges to be solved.
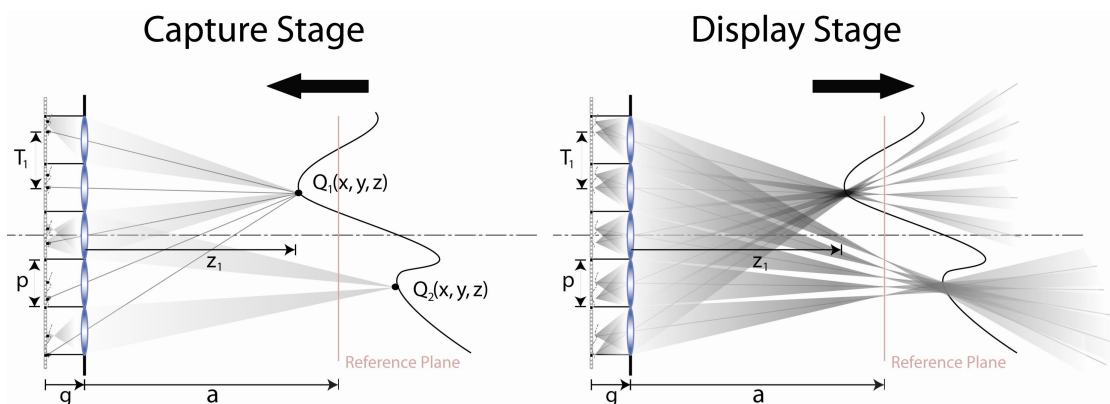

FIGURE 1. Symmetrical capture and display of 3D scenes.

2. INTEGRAL IMAGING: 3D RECONSTRUCTION AND DISPLAY

Integral ImaginIn the InI pickup stage, a microlens array (MLA) generates a set of projections, or microimages, of a 3D scene. These projections are recorded onto a matrix sensor which is located at a distance g from the MLA. Note that, if only these two elements are used, the microimages would be recorded with no limitation in extension. In other words, the microimages provided by neighbouring microlenses overlap. Consequently, a set of opaque barriers must be used to carve up the recording plane into a set of elementary cells. The part of a microimage which falls inside its corresponding elementary cell is known as elemental image. The elemental images is defined as the set of all the recorded elemental images.

By looking the Fig. 1, it is apparent that any point source located at the position $Q(x,y,z)$ generates a set of equally spaced images, namely $\{x'_{mn}\}$, at the positions:

$$\boldsymbol{x}'_{mn} = \left(M_z x + m\, T_z, M_z y + n\, T_z, -g \right), \tag{1}$$

where

$$T_z = \frac{z+g}{z}\, p, \tag{2}$$

$$M_z = -\frac{g}{z}, \tag{3}$$

stand for the z-period of the source and the latelar magnification of the corresponding microimage. Since the extent of the microimages is limited by the opaque barriers, the images will be recorded only if

$$\left| M_z x + m\left(T_z - p \right) \right| < \frac{p}{2}, \tag{4}$$

$$\left| M_z y + n\left(T_z - p \right) \right| < \frac{p}{2}. \tag{5}$$

In the display stage, the integral image is placed in front of a MLA and it is diffusely back-illuminated. If the projection geometry is completely symmetrical to the capture geometry, the rays of light intersect at the original location of the objects that produced the microimages.

3. OBSERVATION GEOMETRY: VIEWING ANGLE.

In the display stage, the observer only sees a small part, or microfacet, of the image formed by each microlens[7]. The composition of all the microfacets provided by the MLA provides the complete field of the scene. This phenomenon is illustrated in Fig. 2. For the sake of simplycity, only the facets corresponding to the microlenses +1 and -2 are drawn. The microfacets are located at the reference plane and their borders are obtained by joining the borders of the corresponding microlens with the center of the pupil of the observer. In this case, the two microfacets provide the images of the two sources in the Fig. 2. The set of all the microfacets forms the final image. When the position of the observer changes, the regions that fall in each microfacet also changes. Consequently, the final image varies according to the relative position of the eye and the object, providing the 3D autostereoscopic image.
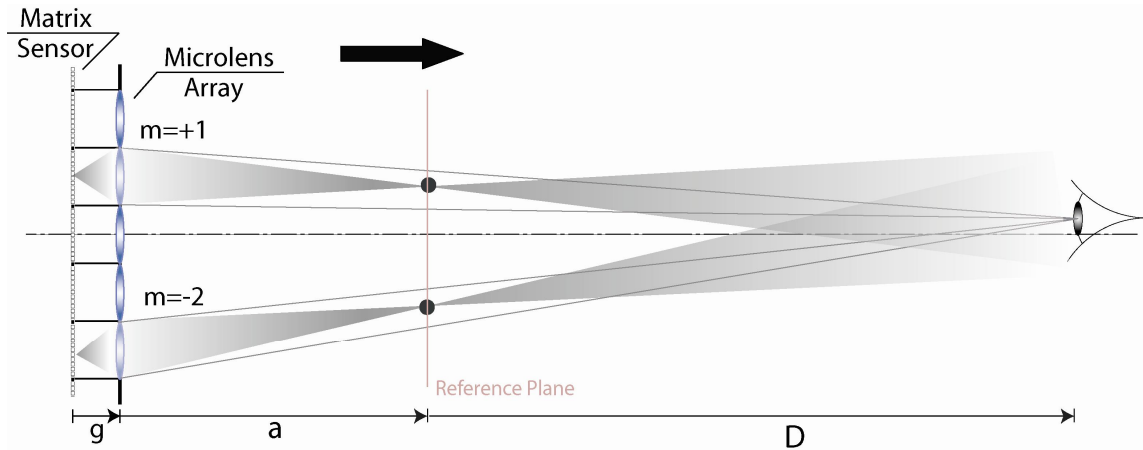
FIGURE 2. Multifacetted structure of the InI display stage. The observer sees a small region of the 3D image through each microlens. The complete image is obtained as the composition of the facets provided by all the microlenses in the array.

Since the image is obtained as the composition of the microfacetes, the field of the observed image depends on the position of the observer. Fig. 3 illustrates this phenomenon. Each microlens provides a microfacet only within a small angle, namely α. Consequently, the observers looking at the display from axially displaced points only can see a small field of the complete scene.
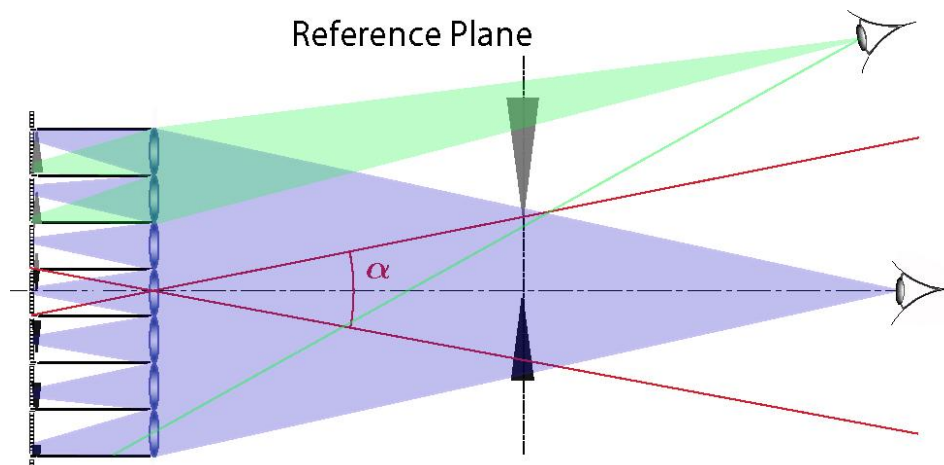
FIGURE 3. The complete scene can be seen only within a very narrow angle know as viewing angle. When the observer looks at the MLA outside the region defined by the viewing angle, he/she observes images provided only by a few microlenses.

4. RELAY OPTICS

Relay optics is commonly used to transport the integral image onto the recording device with proper magnification. The imaging properties of the relay capture system are sketched in Fig. 4. Since each element has a finite size, a vignetting effect is expented on the image that is actually recorded by the sensor[8]. The diaphragm of the relay system usually acts as the aperture stop of the optical setup, while the lens acts as the field stop. Thus, the relay cannot transport the microimage as a whole but only a small region of it, or microvignette. Fig. 4 shows the ray tracing that provides the location and amplitude of the half-illumination and limit fields on the aerial images plane. For the completeness' sake,

the half-illumination and limit fields are also shown on the reference plane. Note that each microvignette is not centered at the optical axis of the corresponding microlens. Indeed, the center of each microvignette is located at

$$\vec{x}_{m,n}^{v} = \frac{s-g}{s} p\,(m,n)\,,\qquad(6)$$

being s the distance between the entrance pupil (EP) of the relay and the MLA. The amplitude of each microvignette, ϕ^{V}, can be computed to be

$$\phi_{m,n}^{V} = \frac{s-g}{s} p\,.\qquad(7)$$

From these equations it is straightforward to induce that the only location of the EP that makes each microvignette to match, both in position and in size, to the corresponding elemental image is infinity[7]. In other words, the relay used in InI has to be necessarily telecentric in the object space.
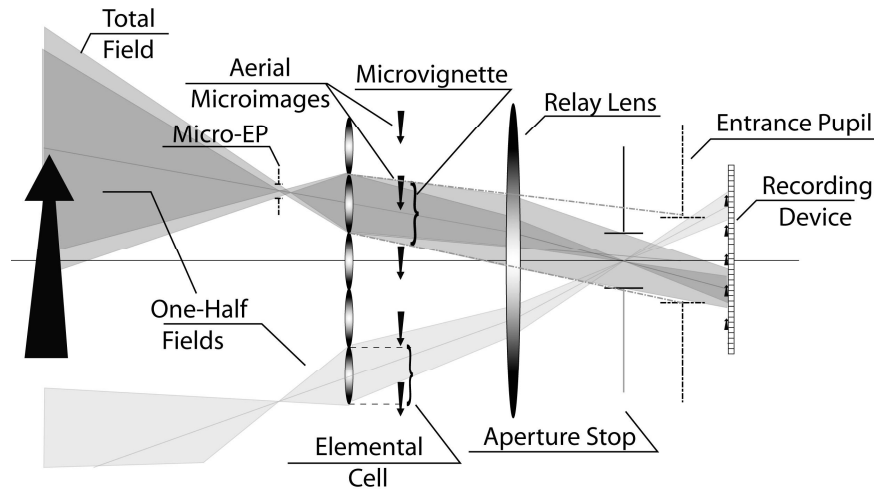
FIGURE 4. Capture setup by using relay optics. The vignetting effect between each microlens and the relay lens limits the extension of the recorded images. In the standard configuration, the total fields corresponding to neighbour elemental images overlap.

Since the limit fields are always greater than the half-illumination ones, the microvignettes corresponding to neighbouring microlenses overlap with each other. Given that the extension of the limit field depends on the diafragm size, a small diaphragm minimizes the overlapping effect. Fig. 5 illustrates the the performance of a telecentric relay with a small aperture. Note that it is possible to convert a non telecentric relay into a telecentric one by using a field lens (FL). The telecentricity condition requires that the EP must be placed at the back focal plane of the FL. In this case, the microvignettes are true scaled versions of the elemental images conforming the integral image.

The telecentric relay system can be used for the display stage as well. The geometry of the projection system is completely symmetrical to the configuration in capture system. In this case, the matrix sensor is replaced by a display device. In the capture setup the optical barriers avoid the overlapping between neighbour elemental images. In the pickup stage, the optical barriers avoid the flipping effect[9].
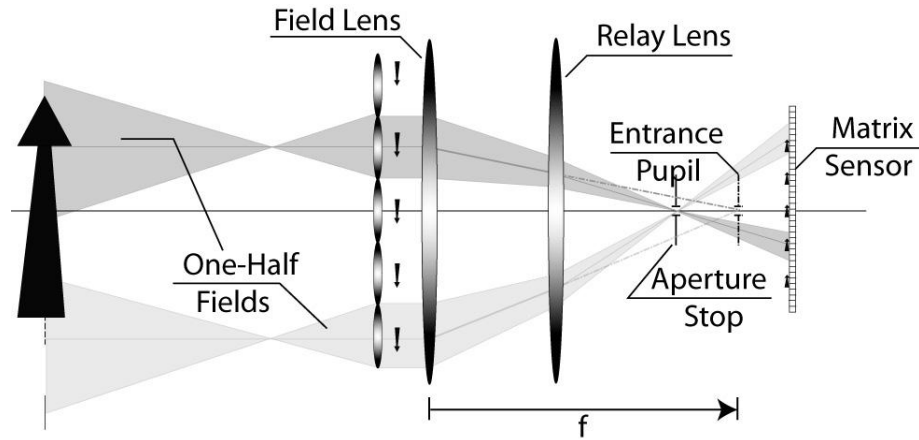
FIGURE 5. Scheme of a telecentric relay system for optimal recording of integral images. The field lens is placed in such a position that its focal plane is located at the entrance pupil of a non-telecentric relay system. In this configuration, the images are recorded exactly as if the matrix sensor was located at the image plane of the MLA.

5. FACET BRAIDING

The formation of 3D images in InI systems can be understood as the composition of three phenomena[10]. First, one must consider the projection of the rays from the integral image through each microlens. The central rays of each cone of rays intersect at the position of the object. Second, each microlens focus the corresponding elemental image on the reference. Finally, the observer sees an image composed of the facets provided by the microlenses.

As it can be seen in Fig. 6.a), there is an agreement between the three above phenomena in the display of images corresponding to objects at the reference plane. Effectively, the rays projected through the microlenses intersect on the reference plane, exactly at the same position as the original point objects. Moreover, the images provided by every microlens are at the same location and have the same size as the original object, since the magnification factor is now exactly the inverse of the magnification in the capture stage. Finally, the observer sees a different part of the image through each microlens. Since the location and the magnification of all of the images coincide, the multifacetted image has a continuous aspect.

In the case of objects outside the reference plane, Figs. 6.b) and c), the projected rays from the integral image through the microlenses intersect, as in the previous case, at the source points that originated them. However, the conjugated plane for the projection plane is still the reference object plane. Consequently, the images provided by the microlenses are shifted between each other and are projected with a magnification factor that is independent from the one in the pickup stage. Finally, when the observer looks at the facetted image, he sees a discontinuous or cracked image (see Fig. 8.d)).

Although the braiding effect is a fundamental drawback of InI displays, it is possible to choose the position of the plane without braiding by controlling the focal of the lenslets in the microlens array. Note that there is no braiding if the system is designed to provide only one pixel per microfacet.
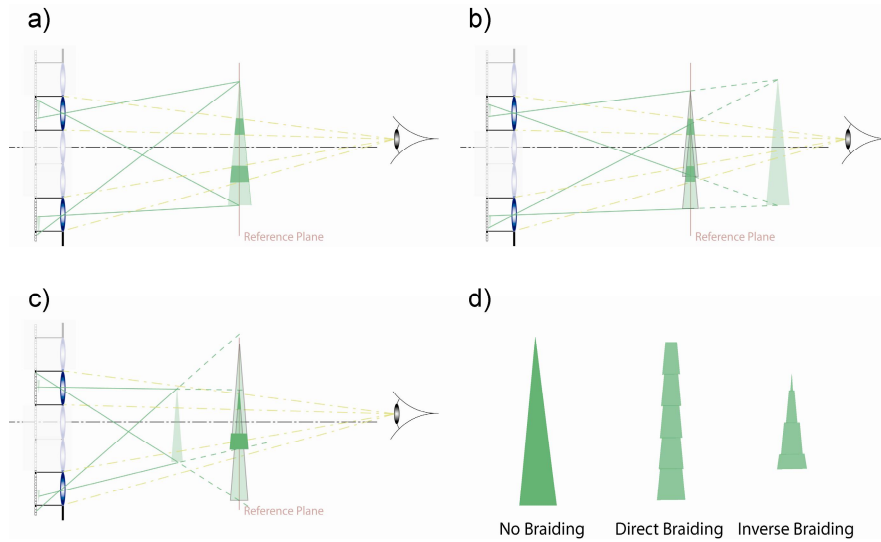
FIGURE 6. Formation of braided images in InI projection systems. The facetted nature of the observation stage is schematized for a) objects at the reference plane, b) objects between the observer and the reference plane and c) between the reference plane and the microlens array. The final images are shown in d). The no-braiding image corresponds to the case a), the direct braiding occurs in the situation b) whereas the inverse braiding happens in the case c).

6. DEPTH OF FIELD IN THE PICKUP STAGE

InI systems are not linear-shift invariant since the impulse response depends on the depth coordinate of the source, z[11]. Therefore, one can not define an impulse response, but a distribution function that describes all the possible responses in the system. Fig. 7.a) shows the meridian section of the distribution function, *H(x, y=0, a-z)*, corresponding to an InI system with $f = 3.3\ mm$, $a = 100\ mm$, $p = 1\ mm$ which is illuminated by a quasimonochromatic source of mean wavelength $\lambda = 550\ nm$. To illustrate the effects of the non linearity we show in Fig. 7.b) one elemental image of such a system. The original 3D scene is composed by four spoke targets placed at different depths.
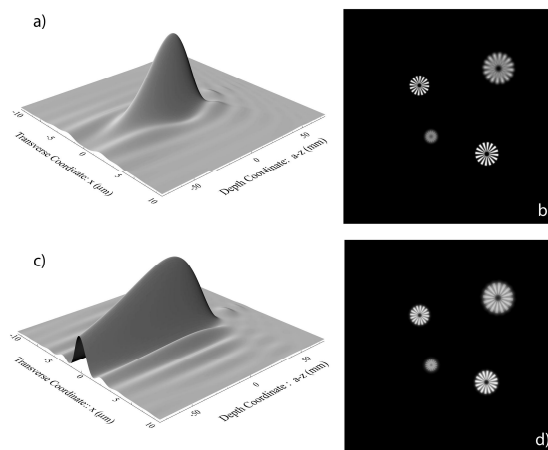
FIGURE 7. Distribution function and the corresponding central elemental image in a standard pickup system (a and b). The shape of the distribution function (c) shows the extension of the depth of field due to the use of apodizing filters. The central elemental image (d) is also shown for comparison purposes.

The performance of the system can be improved by using apodization techniques on the MLA. Simulated elemental images in apodized systems are shown in Figs. 8.c) and d). The depth of field can be increased more efficiently by combining apodization techniques and deconvolution tools[12]. This is possible because the apodization can be used to obtain a quite-invariant distribution function. The deconvolution can be performed by using an effective impulse response in a broad range of depths. Fig. 8 shows the performance of the hybrid technique in a simulated capture system.
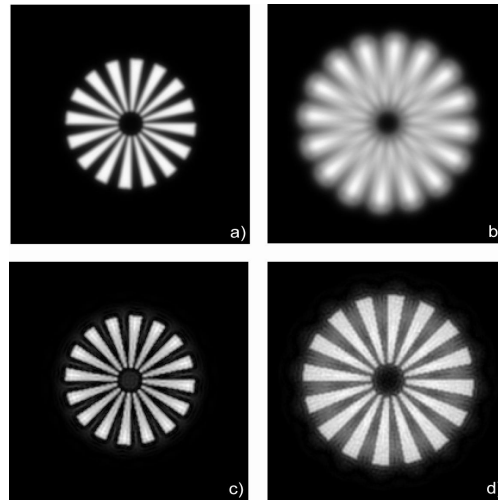
FIGURE 8. Comparison between the images in standard systems (a and b) and the corresponding images using the hybrid technique (c and d).

7. CONCLUSIONS

We analyze the InI technique from the point of view of the optics to improve its performance. The techniques proposed in this proceeding concern some of the main challenges of this technique. The depth of field in the capture stage and the braiding effect strongly limit the applications of these systems. The design of a proper relay for the capture of integral images has been treated as well.

ACKNOWLEDGMENTS

REFERENCES

1. G. Lippmann, "Epreuves reversibles donnant la sensation du relief," J. Phys. **7**, 821–825 (1908).
2. H. E. Ives, "Optical properties of a Lippmann lenticulated sheet", J. Opt. Soc. Am. **21**, 171–176 (1931).
3. F. Okano, H. Hoshino, J. Arai y I. Yuyama, "Real-time pickup method for a three-dimensional image based on integral photography," Appl. Opt. **36**, 1598–1603 (1997).

4. Jang, J.-S. and B. Javidi, "Improved viewing resolution of three-dimensional integral imaging by use of nonstationary micro-optics," Opt. Lett. **27**, 324-326 (2002).

5. R. Martínez-Cuenca, G. Saavedra, M. Martínez-Corral and B. Javidi, "Enhanced depth of field integral imaging with sensor resolution constraints," Opt. Exp. **12**, 5237-5242 (2004).

6. J.-H. Park, H.-R. Kim, Y. Kim, J. Kim, J. Hong, S.-D. Lee, and B. Lee, "Depth-enhanced three-dimensional two-dimensional convertible display based on modified integral imaging," Opt. Lett. **29**, 2734-2736 (2004).

7. M. Martínez-Corral, B. Javidi, R. Martínez-Cuenca and G. Saavedra, "Multifacet structure of observed reconstructed integral images," J. Opt. Soc. Am. A **22**, 597-603 (2005).

8. R. Martínez-Cuenca, A. Pons, G. Saavedra, M. Martínez-Corral and B. Javidi, "Optically-corrected elemental images for undistorted integral image display," Opt. Exp. **14**, 9657–9663 (2006).

9. Byoungho Lee, Sungyong Jung, and Jae-Hyeung Park, "Viewing-angle-enhanced integral imaging by lens switching," Opt. Let. **27**, 818-820 (2002).

10. R. Martínez-Cuenca, G. Saavedra, A. Pons, B. Javidi and M. Martínez-Corral, "Facet braiding: a fundamental problem in Integral Imaging," Opt. Let. **32**, 1078–1080 (2007).

11. M. Martínez-Corral, B. Javidi, R. Martínez-Cuenca and G. Saavedra, "Integral imaging with improved depth of field by use of amplitude-modulated microlens array," Appl. Opt. **43**, 5806-5813 (2004).

12. R. Martínez-Cuenca, G. Saavedra, M. Martínez-Corral and B. Javidi, "Extended depth-of-field 3-D display and visualization by combination of amplitude-modulated microlenses and deconvolution tools," J. Disp. Technol. **1**, 321-327 (2005).